Numerical Analysis of Perforated Microring Resonator Based Refractive Index Sensor

M. Gabalis[*1], D. Urbonas[1], and R. Petruškevičius[1]
[1]Institute of Physics of Center for Physical Sciences and Technology, Vilnius, Lithuania
*gysliukas@micro.lt

Abstract: In this work perforated microring resonator based refractive index sensor is presented. Numerical analysis of the microring using COMSOL Multiphysics was performed. From transmission spectra sensitivity and quality factor of our proposed structure were evaluated. It was shown that perforated microring resonator exhibits higher sensitivity than ordinary microring resonator while also maintaining high quality factor.

Keywords: microring resonator, refractive index sensor.

1. Introduction

Label free, refractive index (RI) based biosensors have recently emerged as one of the most promising optical sensing techniques [1]. Microring resonators have several attractive features for sensing applications. It's high quality factor and multiple pass interaction nature allows to resolve small shifts in resonance wavelength induced by introducing sensing object near the resonator [2, 3]. When a sensing object, having different RI than media that surrounds microring is positioned near the resonator, it induces the change in average refractive index at that location. This in turn changes the resonance condition. This change can be observed as a resonance wavelength shift in the transmission spectra. Monitoring this change allows one to determine the nature of the sensing object. However, ordinary microring resonator does not have high sensitivity. This is mainly attributed to high confinement of light in the guiding material. Several microring geometries aimed at increasing extension of light into the surrounding media have been reported (slotted microring [4, 5], SNOW microring [6]). In this work we present microring resonator with perforated circular holes (figure 1) and numerically analyze its performance in sensing applications.

2. Perforated Microring Resonator

The geometry of the analyzed microring resonator is shown in figure 1. Geometrical parameters of the resonator and waveguide are as follows: outer ring radius 2.15 µm, ring width 0.35 µm, hole radius 0.07 µm, waveguide width 0.25 µm and distance from waveguide to the ring was set to 0.15 µm. Refractive index of the high dielectric material (black color in figure 1) was set to 3.46 and refractive index of low dielectric material was 1.46. To compute the sensitivity we changed refractive index of the low dielectric material to 1.52. Structure was simulated in 2D spatial domain. Coupling to the microring resonator is performed through the waveguide. Excitation source is located at the left side of the waveguide (figure 1). For excitation we used TM polarization source (Magnetic field vector is directed out of the page in figure 1). Simulations were performed in the wavelength window starting from 1.38 µm and ending at 1.43 µm.

In some simulations we also changed radius of one of the holes to 0.047 µm (defect hole in figure 1, right side of the microring resonator).

Performance of microring resonator based refractive index sensor was analyzed by monitoring two parameters: sensitivity (S) and quality factor (Q). Bulk sensitivity refers to change in resonance wavelength divided by change in refractive index of surrounding medium (equation 1).

$$S = \frac{\Delta\lambda}{\Delta n} \tag{1}$$

Quality factor is a dimensionless quantity that expresses the photon lifetime (in cycles) inside the resonator structure. Quality factor can be expressed as follows:

$$Q = \frac{\lambda}{\Delta\lambda} \tag{2}$$

We will also refer in the text to resonance condition of the microring resonator:

$$2\pi R n_{eff} = m\lambda_r \tag{3}$$

Where R is radius of the ring, n_{eff} - effective refractive index of microring core, m - positive integer, λ_r - resonance wavelength. Equation 3 says that for resonance to occur optical path in the resonator must be equal to integer multiple of the wavelength.

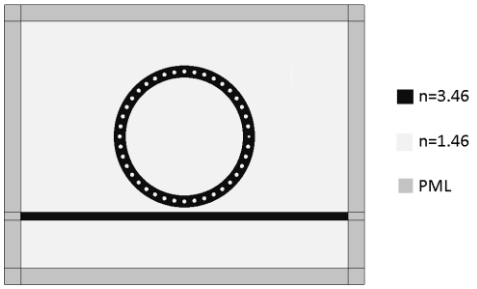

Figure 1. Geometry of the analyzed perforated microring resonator.

3. Use of COMSOL Multiphysics

COMSOL was used to solve Helmholtz equation (equation 4) in 2D spatial domain for the structure shown in figure 1. Excitation source having spatial distribution of fundamental waveguide mode was set at left side of the waveguide. Transmitted power was monitored at the right side of the waveguide. To get a transmission spectra, wavelength of the excitation source was set as a parameter and parametric sweep for different wavelengths was performed. To suppress any reflection from boundaries of computation window, perfectly matched layers were used (figure 1).

Mesh used in simulations is shown in figure 2.

$$\nabla \times \left(\left(\varepsilon_r - \frac{j\sigma}{\omega_0 \varepsilon_0} \right) \nabla \times \vec{H} \right) - \mu_r k_0^2 \vec{H} = 0 \quad (4)$$

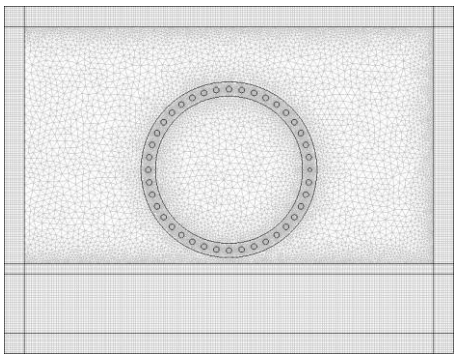

Figure 2. Mesh used in simulations.

4. Results

Transmission spectra of the microring resonator with equal holes and of the microring resonator with one defect hole is shown in figure 3. Since perforated microring resonator can be regarded as modification of holey waveguide (7) we see a band gap starting from 1.405 μm. When we modify radius of one hole defect mode positioned at λ=1.4156 μm appears in the transmission spectra. From data shown figure 3 we can calculate quality factor for different resonance wavelengths. The two resonance of microring with equal holes have resonance wavelengths of 1.3955 μm and 1.4048 μm and Q factors of 1812 and 2431 respectively. As can be seen from figure 3, microring with equal holes and microring with one defect hole have same resonance at 1.3955 μm. The other two resonances for microring with defect hole occurs at 1.4003 μm and 1.4156 μm. Their Q factors are 2729 and 3146.

We evaluated sensitivity in three different ways. For bulk sensitivity we changed the refractive index of low dielectric material from 1.46 to 1.52. So that shift of 0.06 refractive index units (RIU) results. Secondly we only changed refractive index inside the holes from 1.46 to 1.52. And third - refractive index inside the defect hole was changed from 1.46 to 1.52.

Transmission spectra from which bulk sensitivity was evaluated is shown in figure 4. Comparison with figure 3 shows that resonance wavelengths have shifted towards longer wavelengths. This is expected result. One can see from equation 3 than increasing effective refractive index of core material results in increase in resonance wavelength. When one increases refractive index of low dielectric material around the resonator and inside the holes one also increases effective refractive index of microring core material. However increasing refractive index of the low dielectric material also results in lowering Q factor values. Sensitivity evaluated using equation 2 is 264 nm/RIU for both microrings with equal holes and with defect hole. Ordinary microring resonator (by this we mean microring resonator without perforations) has bulk sensitivity of about 80 nm/RIU.

Transmission spectra for microring for which only refractive index inside the holes was changed is shown in figure 5. As one would

expect shifts in resonance wavelengths are smaller than in the previous case. In this case we cannot express the sensitivity using equation 2 since it is for bulk sensitivity. Shifts in resonance wavelengths are 7.4 nm for both microring with equal holes and for microring with one defect hole.

In figure 6 transmission spectra for defect hole microring resonator is shown. Two lines represent different refractive indices of defect hole. One is for case in which refractive index of the defect hole is same as of all the other holes and surrounding medium. Second is for case when refractive index of defect hole is increased to 1.52. One can see from figure 6 than increasing refractive index of the defect hole has no effect on resonance position of first two visible resonances. However there is observable shift in defect mode resonance wavelength. From data shown in figure 6 this shift is evaluated to be equal to 0.6 nm.

Magnetic field distributions under the resonance conditions are presented in figures 7-11. From these figures one can see mode field profiles at different resonance wavelengths and get some insight into the results regarding transmission spectra and sensitivity. From figure 3 it is seen that microring resonator with equal holes and microring resonator with one defect hole both have same resonance wavelength of 1.3955 μm. From figures 7 and 9 it is seen that both modes have similar spatial distribution and that field is concentrated at upper and lower parts of the microring. So introducing a defect hole does not effect this mode noticeably.

Resonance at 1.4048 μm in microring with equal defects and resonance at 1.4003 μm in microring with one defect hole have different spatial field distributions (figure 8 and figure 10) and so their resonance wavelengths are different. Mode for microring with one defect hole has shifted towards lower wavelength in comparison with microring resonator with equal holes (figure 3).

In figure 11 field distribution at resonance wavelength 1.4156 for microring resonator with one defect hole is shown. This mode represent a defect mode shown in figure 3. It's field is concentrated around the defect hole. So it's only this mode that is affected by changing refractive index of the defect hole (figure 6).

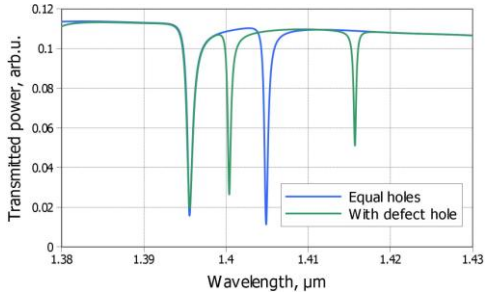

Figure 3. Transmission spectra of perforated microring resonator.

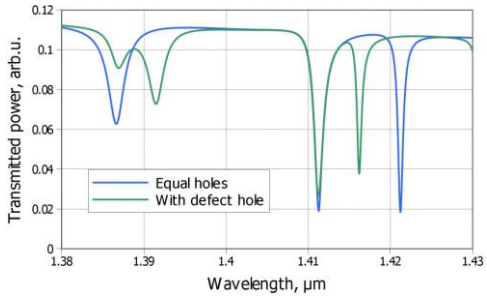

Figure 4. Transmission spectra of microring resonators when refractive index of low dielectric material was shifted from 1.46 to 1.52.

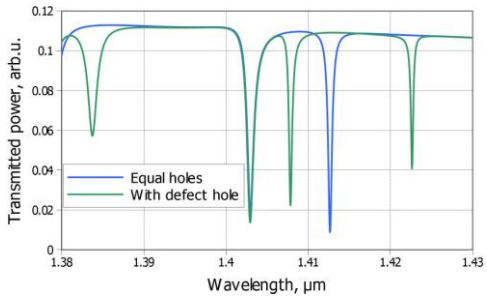

Figure 5. Transmission spectra of microring resonators when refractive index of holes was shifted from 1.46 to 1.52.

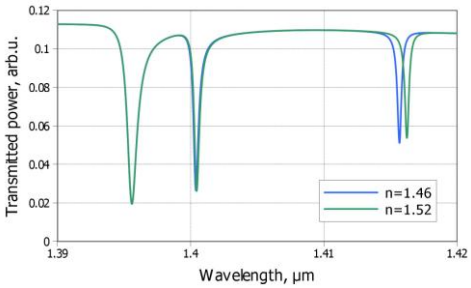

Figure 6. Transmission spectra of microring resonator with defect hole when refractive index of the defect hole material is 1.46 and 1.52.

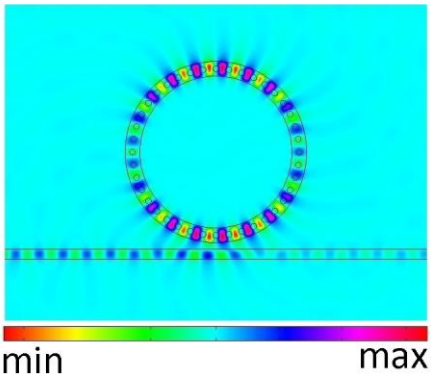

Figure 7. Magnetic field distribution. Microring resonator with equal holes. Wavelength is 1.3955 μm.

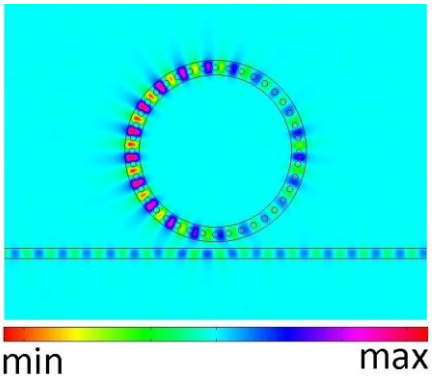

Figure 8. Magnetic field distribution. Microring resonator with equal holes. Wavelength is 1.4048 μm.

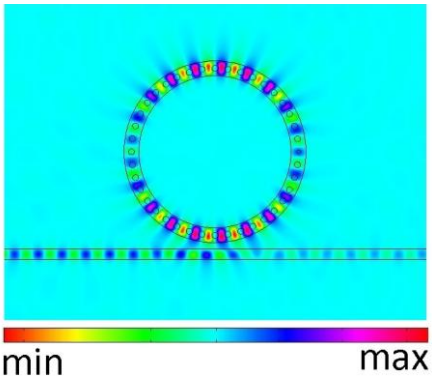

Figure 9. Magnetic field distribution. Microring resonator with defect hole. Wavelength is 1.3955 μm.

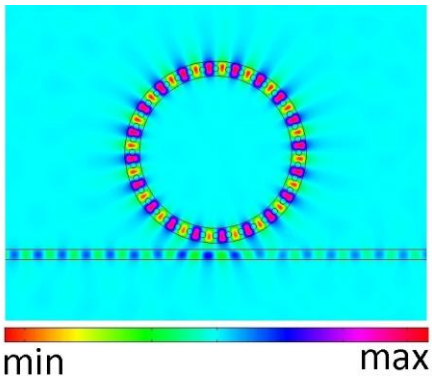

Figure 10. Magnetic field distribution. Microring resonator with defect hole. Wavelength is 1.4003 μm.

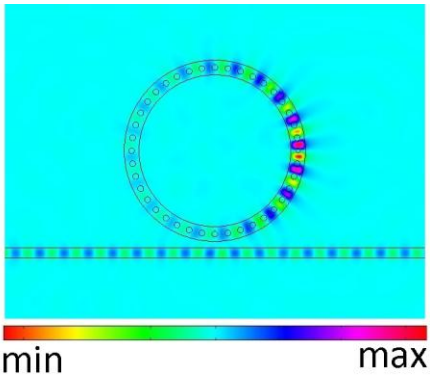

Figure 11. Magnetic field distribution. Microring resonator with defect hole. Wavelength is 1.4156 μm.

5. Conclusions

We have presented perforated microring resonator based refractive index sensor and analyzed its performance. It was shown that our design has higher sensitivity than ordinary microring resonator. Our future work will include simulations of same structure in 3D spatial domain and numerical analysis of the resonator performance in single particle detection setup.

6. Acknowledgements

This project is funded by the Republic of Lithuania and European Social Fund under the 2007-2013 Human Resources Development Operational Programme's priority 3. (VP1-3.1-SMM-10-V-02-026).

7. References

1. M. S. Luchansky, R. C. Bailey, High-Q Optical Sensors for Chemical and Biological Analysis, *Analytical Chemistry*, **84**, 793-821 (2012)
2. C. A. Barrios, Integrated microring resonator sensor arrays for labs-on-chips, *Analytical and Bioanalytical Chemistry*, **403**, 1467-1475 (2012)
3. C. Chao, A. Arbor et al., Design and optimization of microring resonators in biochemical sensing applications, *Lightwave Technology*, **24**, 1395-1402 (2006)
4. K. R. Hiremath, J. Niegemann, K. Busch, Analysis of light propagation in slotted resonator based systems via coupled-mode theory, *Optics Express*, **19**, 8641-8655 (2011)
5. C. A. Barrios, K. B. Gylfason, et al., Slot-waveguide biochemical sensor, *Optics Letters*, **32**, 3080-3082 (2007)
6. M. Khorasaninejad, N. Clarke, et al., Optical bio-chemical sensors on SNOW ring resonators, *Optics Express*, **19**, 17575-17584 (2011)
7. S. Fan, J. N. Winn, A. Devenyi, et al., Guided and defect modes in periodic dielectric waveguides, *Journal of the Optical Society of America B*, **12**, 1267-1272 (1995)